Politecnico di Milano

Spacecraft Attitude Dynamics and Control

Space Engineering

Final Project
Micro-spacecraft - GEO

Student:
Gonçalo Eduardo Cascalho Raposo
10670412

Professor:
James Douglas Biggs

January 12, 2019

Contents

1 Mission **1**
1.1 Mission phases . . . 1
1.1.1 De-tumbling . . . 1
1.1.2 Slew maneuver . . . 1
1.1.3 Tracking . . . 2
1.2 Orbit . . . 2
1.3 Spacecraft . . . 2
1.3.1 Dimensions . . . 2
1.3.2 Sensors . . . 3
1.3.3 Actuators . . . 4
1.3.4 Table . . . 5
1.3.5 ADCS architecture . . . 5

2 Modeling **6**
2.1 Dynamics . . . 6
2.2 Attitude . . . 7
2.3 Orbit . . . 8
2.3.1 A_{LN} matrix . . . 8
2.3.2 $\vec{r}$ vector . . . 8
2.3.3 Sun vector $\vec{S}$ . . . 9
2.3.4 Relative velocity $\vec{V_r}$ . . . 9
2.3.5 Magnetic field $\vec{B}$ . . . 9
2.3.6 Earth horizon vector $\vec{EH}$ . . . 10
2.4 Disturbances . . . 10
2.4.1 Gravity gradient . . . 11
2.4.2 Solar radiation pressure . . . 11
2.4.3 Parasitic magnetic torque . . . 11
2.4.4 Drag . . . 12
2.5 Sensors . . . 12
2.5.1 Gyroscope . . . 12
2.5.2 Magnetometer . . . 12
2.5.3 Earth horizon sensor . . . 13
2.5.4 Gyroscope noise filtering . . . 13
2.5.5 Attitude determination . . . 13
2.6 Controller . . . 14
2.6.1 De-tumble controller . . . 14
2.6.2 Slew maneuver and tracking controller . . . 15
2.6.3 Switching controllers . . . 15
2.7 Actuators . . . 16
2.7.1 CG thrusters . . . 16
2.7.2 Reaction wheels . . . 16
2.7.3 Estimated control torques . . . 17

3 Results **18**

Chapter 1

Mission

The assigned mission consisted of a micro-spacecraft in a geosynchronous equatorial orbit (GEO). The spacecraft is required to perform inertial pointing, as in star pointing, for example.

1.1 Mission phases

The mission can then be divided into three phases: de-tumbling, slew maneuver, and tracking.

1.1.1 De-tumbling

When the spacecraft is inserted into orbit, it may have an undesired spin (angular velocity). In order to accomplish the mission requirements, the spacecraft should first be taken into a stop, reducing its velocity to zero (or close to it).

Therefore, the de-tumbling part of the mission is characterized by:

$$\vec{\omega}(0) = \vec{\omega}_0 \qquad \vec{\omega}(t) \to 0 \tag{1.1}$$

where the vector $\vec{\omega}$ is the angular velocity of the spacecraft and $\vec{\omega_0}$ is the initial angular velocity, which may be unknown.

In the assigned mission, the spacecraft should do the de-tumbling with a gyroscope as a sensor and 4 cold gas (CG) thrusters as actuators.

1.1.2 Slew maneuver

Having the spacecraft with zero velocity, it may have any given attitude. The objective of this phase is to point the spacecraft to a given point, with zero final velocity.

The slew maneuver is characterized by:

$$\vec{\omega}(0) = 0 \qquad \vec{\omega}(t) \to 0 \tag{1.2}$$

$$\vec{q}(0) = \vec{q}_0 \qquad \vec{q}(t) \to \vec{q}_d \tag{1.3}$$

where the vector $\vec{q}$ is the attitude of the spacecraft, represented by a quaternion, and $\vec{q_0}$ is the attitude after the de-tumbling, which may be unknown.

In this phase of the mission, the spacecraft should use the gyroscope and a magnetometer as sensors and 3 reaction wheels (RW) as actuators.

1.1.3 Tracking

This phase consists in tracking a desired velocity and attitude. One example could be an imaging satellite that was desired to point at the Earth's surface.

The tracking is characterized by:

$$\vec{\omega}(t) = \vec{\omega}_d(t) \tag{1.4}$$

$$\vec{q}(t) = \vec{q}_d(t) \tag{1.5}$$

where $\vec{\omega}_d$ is the desired angular velocity, that can change in time, and q_d is the desired attitude quaternion, which can also change in time.

Since the desired angular velocity is zero, then the tracking can be treated simultaneously with the slew maneuver.

1.2 Orbit

The orbit is a geosynchronous equatorial orbit (GEO), also known as geostationary orbit. This type of orbit is characterized by a period of exactly one sideral day and an inclination of $0°$. The orbital parameters: orbital angular velocity n, orbit radius R and orbital velocity v can be calculated as follows:

$$n = \frac{2\pi}{T} \simeq 7.2921 \times 10^{-5}\,\mathrm{rad/s} \tag{1.6}$$

with T being the orbital period, $T = 86164.09\,\mathrm{s}$.

$$R = \sqrt[3]{\frac{\mu_\oplus}{n^2}} \simeq 4.2164e \times 10^4\,\mathrm{km} \tag{1.7}$$

with $\mu_\oplus$ being the Earth's gravitational parameter, $\mu_\oplus = 3.986 \times 10^5\,\mathrm{km}^3/\mathrm{s}^2$.

$$v = \sqrt{\frac{\mu_\oplus}{R}} \simeq 3.0747\,\mathrm{km/s} \tag{1.8}$$

1.3 Spacecraft

The only information about the assigned spacecraft is that it is a micro-spacecraft. A rough description of a micro-spacecraft is that it has a mass between 10 and 100 kg [1]. However, the term can sometimes refer to satellites larger or smaller than that.

The spacecraft modeled was assumed to have a shape similar to the ESA satellite: *PROBA-V*.

1.3.1 Dimensions

The PROBA-V is a satellite from the European Space Agency (ESA). The most important dimensions are [2]:

- Mass $= m_s = 138\,\text{kg}$
- Dimensions $= 765 \times 730 \times 830\,\text{mm}$
- $I_x = \dfrac{1}{12}m(b^2 + c^2) \approx 14.05\,\text{kgm}^2$
- $I_y = \dfrac{1}{12}m(a^2 + c^2) \approx 14.65\,\text{kgm}^2$
- $I_z = \dfrac{1}{12}m(a^2 + b^2) \approx 12.86\,\text{kgm}^2$

where the moments of inertia were estimated for an homogeneous cuboid shaped body.

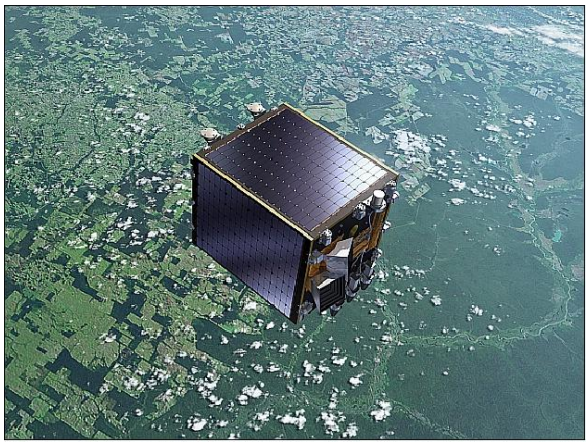

Figure 1.1: *PROBA-V* spacecraft in orbit [2].

1.3.2 Sensors

The sensors to be used in the mission are a gyroscope and a magnetometer. However, a Earth horizon sensor was added to make the system observable. A brief description of the instruments is presented below.

Gyroscope

The selected gyroscope was the *Sensonor STIM300*. Its datasheet can be found in [3], but the main characteristics are:

- Mass $= m_g = 0.055\,\text{kg}$
- Dimensions $= 38.6 \times 35.9 \times 21.5\,\text{mm}$
- Power $= P_g = 1.5 \sim 2.0\,\text{W}$
- Sampling frequency $= f_s = 262\,\text{Hz}$ (max: $2\,\text{kHz}$)
- Low gyro noise $= ARW = 0.15\,^\circ/\sqrt{\text{h}}$
- Low gyro bias instability $= \dfrac{RRW}{\sqrt{T_s}} = 0.3\,^\circ/\text{h}$

where ARW is the angular random walk and RRW is the rate random walk.

Figure 1.2: Gyroscope *Sensonor STIM300* [3].

Magnetometer

The modeled magnetometer was based in the *NSS Magnetometer* [4]. However, the accuracy of the sensor was assumed accordingly to the lecture notes [5]:

- Mass $= m_m = 0.085\,\text{kg}$
- Dimensions $= 96 \times 43 \times 17\,\text{mm}$
- Power $= P_m = 0.750\,\text{W}$
- Accuracy $= e_m = 5\,^\circ$

Figure 1.3: *NSS Magnetometer* [4].

Earth horizon sensor

The Earth horizon sensor was included in the sensors because the orbit is GEO and, therefore, the magnetometer always returns the same reading. In order for the system to be observable, one more sensor needs to be used.

The modeled Earth horizon sensor was based in the *MAI-SES IR Earth Sensor* [6]. However, the accuracy of the sensor was assumed accordingly to the lecture notes [5]:

- Mass $= m_h = 0.033\,\text{kg}$
- Dimensions $= 43.4 \times 31.8 \times 31.8\,\text{mm}$
- Power $= P_h = 0.132\,\text{W}$
- Accuracy $= e_h = 6\,\text{arcmin}$

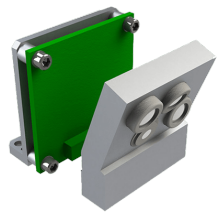

Figure 1.4: *MAI-SES IR Earth Sensor* [6].

1.3.3 Actuators

The actuators available in this mission were 4 cold gas thrusters and 3 reaction wheels.

Cold gas thrusters

The modeled cold gas (CG) thrusters were based in the *VACCO Hybrid ADN Delta-V / RCS System* [7]. However, the distance between nozzles and the thrust were assumed to be 10 times greater, in order for the de-tumble to be faster. For attitude control, only the 4 smaller thrusters are used.

- Mass $= m_t = 1.797\,\text{kg}$
- Dimensions $= 57.00 \times 350.2 \times 350.2\,\text{mm}$
- Power $= P_t = 15\,\text{W}$ (standby: $0.055\,\text{W}$)
- Thrust $= F_t = 100\,\text{mN}$
- Minimum Impulse Bit = MIB $= 0.1\,\text{mNs}$

Figure 1.5: Thrusters *VACCO Hybrid ADN Delta-V / RCS System* [7].

The thrusting system was placed as shown in Figure 1.6 and the dimensions of the thrusting system are in Figure 1.7.

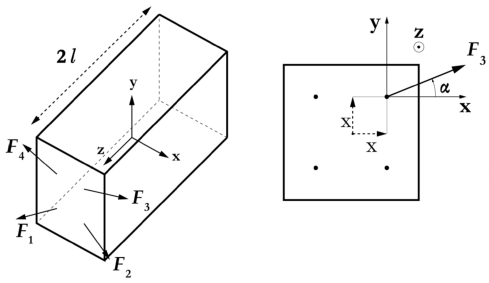

Figure 1.6: Location of the thrusters in the spacecraft [5].

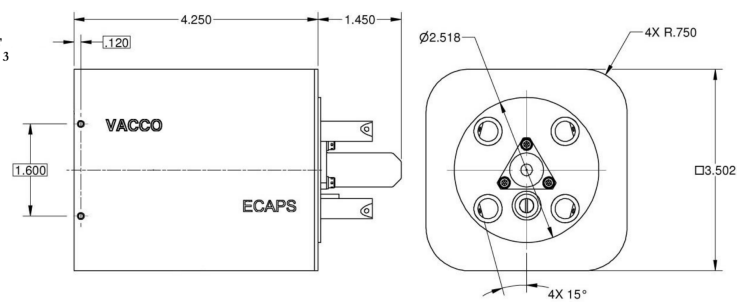

Figure 1.7: Dimensions of the thrusters, in cm [7].

Reaction wheels

In this mission, 3 reaction wheels (RW) were used. They were placed with the axes of rotation aligned with each principal axis of inertia. Since *PROBA* missions used *Rockwell* reaction wheels, the simulated reaction wheels were based in the *RSI 12-75/60* [8].

- Mass $= m_r = 4.85\,\text{kg}$
- Dimensions $= 247 \times 247 \times 85\,\text{mm}$
- Power $= P_r = 20 \sim 90\,\text{W}$
- Maximum angular momentum $= h_r = \pm 12\,\text{Nms}$
- Maximum torque $= \pm 75\,\text{mNm}$

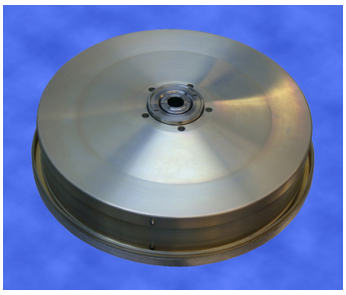

Figure 1.8: *Rockwell RSI 12 Reaction Wheel.* [8]

1.3.4 Table

Table 1.1: Sensors and actuators mass, power and volume.

Components	#	Mass [kg]	Total Mass [kg]	Power [W]	Total Power [W]	Volume [cm3]	Total Volume [cm3]
Gyroscope	1	0.055	0.055	2	2	29.8	29.8
Magnetometer	1	0.085	0.085	0.75	0.75	70.2	70.2
Earth horizon sensor	1	0.033	0.033	0.132	0.132	43.9	43.9
CG thrusters	4	1.797	1.797	15	15	6982	6982
Reaction wheels	3	4.85	14.55	90	270	4073	12220
TOTAL	-	-	16.52	-	287.9	-	19346
TOTAL margin (10%)	-	-	18.17	-	316.7	-	21280

1.3.5 ADCS architecture

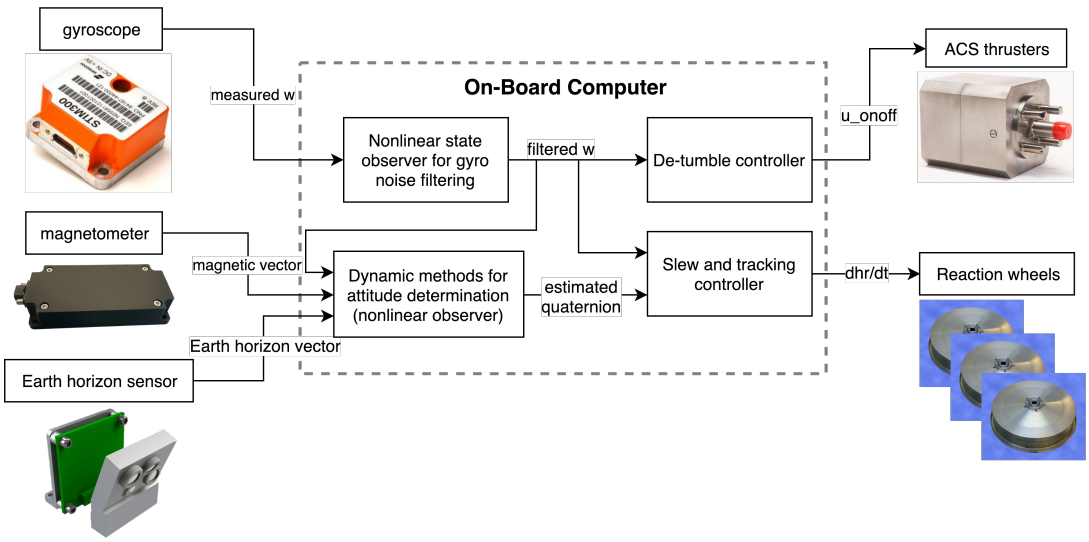

Figure 1.9: ADCS architecture.

Chapter 2

Modeling

To model this system and the mission, a Simulink model was developed. It was divided into multiple subsystems: dynamics, attitude, orbit, disturbances, sensors, controller and actuators. Each of these subsystems will be described in the following sections.

2.1 Dynamics

The dynamics of the spacecraft can be described by the Euler's equations for rigid body motion.

To derive the equations suppose a body with angular momentum defined as

$$\vec{h} = J\vec{\omega} \tag{2.1}$$

where J is the moment of inertia and $\vec{\omega}$ the angular velocity of the body.

By Newton's second law, in an inertial frame N

$$\left.\frac{\mathrm{d}\vec{h}}{\mathrm{d}t}\right|_N = \vec{M} \tag{2.2}$$

where $\vec{M}$ is the external torque.

Changing to a rotating frame B (fixed with the body), the equation becomes

$$\left.\frac{\mathrm{d}\vec{h}}{\mathrm{d}t}\right|_N = \left.\frac{\mathrm{d}\vec{h}}{\mathrm{d}t}\right|_B + \omega \times \vec{h} = \vec{M} \tag{2.3}$$

$\vec{M}$ is the external torque and, assuming that the only acting torques are from disturbances and the ones caused by the spacecraft for control, then it can be decomposed in two components: $\vec{u}_d$ and $\vec{u}_c$. Noting the definition of $\vec{h}$, then the form of the Euler's equations applied in this simulation is derived

$$J\dot{\vec{\omega}} = J\vec{\omega} \times \vec{\omega} + \vec{u}_d + \vec{u}_c \tag{2.4}$$

If the body reference frame is aligned with the principal axes of inertia, then each component of $\dot{\vec{\omega}}$ can be written as

$$\begin{cases} \dot{\omega}_x = \dfrac{(I_y - I_z)\,\omega_y\omega_z + u_{dx} + u_{cx}}{I_x} \\ \dot{\omega}_y = \dfrac{(I_z - I_x)\,\omega_x\omega_z + u_{dy} + u_{cy}}{I_y} \\ \dot{\omega}_z = \dfrac{(I_x - I_y)\,\omega_x\omega_y + u_{dz} + u_{cz}}{I_z} \end{cases} \tag{2.5}$$

This system of equations is integrated in Simulink, in the block *Dynamics*, thus obtaining the angular motion of the spacecraft.

2.2 Attitude

To describe the attitude of the spacecraft, quaternions were used. Quaternions are vectors in $\mathbb{R}^4$ that can describe the attitude of a body. Suppose a body that is subjected to a rotation of ϕ around the axis (e_1, e_2, e_3). This rotation can be represented by the quaternion:

$$\begin{cases} q_1 = e_1 \sin\left(\frac{\phi}{2}\right) \\ q_2 = e_2 \sin\left(\frac{\phi}{2}\right) \\ q_3 = e_3 \sin\left(\frac{\phi}{2}\right) \\ q_4 = \cos\left(\frac{\phi}{2}\right) \end{cases} \tag{2.6}$$

Notice how the quaternion is normalized, that is

$$q_1^2 + q_2^2 + q_3^2 + q_4^2 = 1 \tag{2.7}$$

It's also useful to divide the quaternion q into a vector part $\underline{q}$ and a scalar part q_4:

$$\underline{q} = (q_1, q_2, q_3) \qquad , \qquad q_4 \tag{2.8}$$

Quaternions are very useful to describe rotations since they don't have any singularities, so they are able to describe large amplitude rotations with no problems.

However, it's not straightforward to get a sense of the attitude of the spacecraft just by looking at their values. It's therefore useful to relate quaternions and the direct cosine matrix (DCM). The lines of this matrix correspond to the vector components of the reference frame. The relation is

$$A_{BN} = \left(q_4^2 - \underline{q}^T \underline{q}\right) I + 2\underline{q}\underline{q}^T - 2q_4[\underline{q}\wedge] \tag{2.9}$$

where I is the identity matrix of size 3, and $[\underline{q}\wedge]$ is the matrix that results from the hat operator applied to $\underline{q}$

$$[\underline{q}\wedge] = \begin{bmatrix} 0 & -q_3 & q_2 \\ q_3 & 0 & -q_1 \\ -q_2 & q_1 & 0 \end{bmatrix} \tag{2.10}$$

The inverse transformation, that is, from the DCM matrix to a quaternion, is not singular and can be represented with 4 different sets of alternative equations. However, since they weren't used in this simulation, they won't be presented here, but they can be found in the lecture notes [5].

One important property of quaternions is that the symmetric of a quaternion represents exactly the same attitude. That can be easily seen by equation 2.6. Suppose that the axis of rotation is the same, but the considered angle of rotation is $\phi - 2\pi$, which represents the same final attitude. The resulting quaternion is

$$\begin{cases} q_1 = e_1 \sin\left(\frac{\phi-2\pi}{2}\right) \\ q_2 = e_2 \sin\left(\frac{\phi-2\pi}{2}\right) \\ q_3 = e_3 \sin\left(\frac{\phi-2\pi}{2}\right) \\ q_4 = \cos\left(\frac{\phi-2\pi}{2}\right) \end{cases} \Leftrightarrow \begin{cases} q_1 = e_1 \sin\left(\frac{\phi}{2} - \pi\right) \\ q_2 = e_2 \sin\left(\frac{\phi}{2} - \pi\right) \\ q_3 = e_3 \sin\left(\frac{\phi}{2} - \pi\right) \\ q_4 = \cos\left(\frac{\phi}{2} - \pi\right) \end{cases} \Leftrightarrow \begin{cases} q_1 = -e_1 \sin\left(\frac{\phi}{2}\right) \\ q_2 = -e_2 \sin\left(\frac{\phi}{2}\right) \\ q_3 = -e_3 \sin\left(\frac{\phi}{2}\right) \\ q_4 = -\cos\left(\frac{\phi}{2}\right) \end{cases} \tag{2.11}$$

From the DCM matrix kinematics

$$\dot{A}_{B/N} = -[\vec{\omega}\wedge]A_{B/N} \tag{2.12}$$

the quaternion kinematics can be obtained by simply substituting Eq. 2.9 in Eq. 2.12. One obtains

$$\begin{bmatrix} \dot{q}_1 \\ \dot{q}_2 \\ \dot{q}_3 \\ \dot{q}_4 \end{bmatrix} = \frac{1}{2} \begin{bmatrix} 0 & \omega_3 & -\omega_2 & \omega_1 \\ -\omega_3 & 0 & \omega_1 & \omega_2 \\ \omega_2 & -\omega_1 & 0 & \omega_3 \\ -\omega_1 & -\omega_2 & -\omega_3 & 0 \end{bmatrix} \begin{bmatrix} q_1 \\ q_2 \\ q_3 \\ q_4 \end{bmatrix} \tag{2.13}$$

This system of equations is integrated in Simulink, in the block *Attitude*, thus obtaining the attitude of the spacecraft. In every iteration, the quaternion is normalized, in order to respect Eq. 2.7. The quaternion is also converted to the DCM matrix through Eq. 2.9.

2.3 Orbit

In Simulink, the block *Orbit* computes the A_{LN} matrix, the vector $\vec{r}$, the Sun vector $\vec{S}$, the spacecraft's relative velocity vector with respect to Earth's atmosphere $\vec{V_r}$, the magnetic field $\vec{B}$ and the Earth horizon vector $\vec{EH}$. Each of those will be explained in detail in the following subsections.

2.3.1 A_{LN} matrix

The matrix A_{LN} describes the local-vertical local-horizon (LVLH) reference frame with respect to the inertial frame centered in the Earth.

In the case of a circular orbit, the x axis of the LVLH frame is aligned with the orbit radius vector (the direction from the Earth to the spacecraft), the y axis is aligned with the velocity vector, and the z axis is aligned with the angular momentum vector, which is perpendicular to the previous two.

The A_{LN} matrix can be simply constructed as

$$A_{LN} = \begin{bmatrix} \frac{\vec{r}}{\|\vec{r}\|} & \frac{\vec{v}}{\|\vec{v}\|} & \frac{\vec{r}\times\vec{v}}{\|\vec{r}\times\vec{v}\|} \end{bmatrix}^T \tag{2.14}$$

with $\vec{r}$ and $\vec{v}$ written in the inertial frame. In the case of a circular, equatorial orbit, the vectors can be substituted and one obtains the following matrix

$$A_{LN}(t) = \begin{bmatrix} \cos(nt) & \sin(nt) & 0 \\ -\sin(nt) & \cos(nt) & 0 \\ 0 & 0 & 1 \end{bmatrix} \tag{2.15}$$

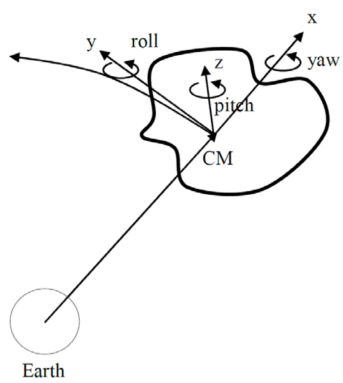

Figure 2.1: Local-vertical local-horizon frame. Described by matrix A_{LN}.

2.3.2 $\vec{r}$ vector

The vector $\vec{r}$ is the unitary vector from the Earth to the spacecraft. In the case of a circular orbit, it can be simply computed, in the inertial frame, as

$$\vec{r}_N = \begin{bmatrix} \cos(nt) & \sin(nt) & 0 \end{bmatrix}^T \tag{2.16}$$

This is also equivalent to obtaining the first line of the A_{LN} matrix. To obtain the vector written in the body frame (frame fixed with the spacecraft), one simply has to multiply the vector by the A_{BN} matrix.

$$\vec{r}_B = A_{BN} \cdot \vec{r}_N \tag{2.17}$$

2.3.3 Sun vector $\vec{S}$

The Sun vector is necessary to compute the solar radiation pressure (SRP).

In the inertial frame (centered in the Earth), the Sun vector can be calculated as

$$\vec{S}_N = \begin{bmatrix} \cos(n_s t + B) \\ \sin(n_s t + B)\cos(ep) \\ \sin(n_s t + B)\sin(ep) \end{bmatrix} \tag{2.18}$$

where n_s is the angular velocity of the Earth around the Sun, B is an initial phase for the position of the Earth in its orbit and ep is the ecliptic inclination.

To get the Sun vector in the body frame, one only has to multiply by the A_{BN} matrix, as in Eq. 2.17.

2.3.4 Relative velocity $\vec{V}_r$

The relative velocity $\vec{V}_r$ is the velocity of the spacecraft with respect to the Earth's atmosphere. This velocity is important to calculate the drag caused by the atmosphere on the spacecraft.

Despite the atmospheric drag not being very important in this problem, since the altitude of the orbit is very high and one may neglect the existence of a thin atmosphere, the modeling will be included so that the model can be applied to different orbits.

Assuming that the Earth's atmosphere rotates with the Earth like a rigid body, then the velocity of the atmosphere would be

$$\vec{v}_{atm} = \vec{\omega}_E \times \vec{R}_n \tag{2.19}$$

where $\vec{\omega}_E$ is the Earth's rotational velocity and $\vec{R}_n$ the position of the spacecraft.

The spacecraft's velocity vector can be obtained by the A_{LN} matrix, where the second row corresponds to the velocity vector. The vector can be calculated as

$$\vec{v}_N = v \cdot ([0 \quad 1 \quad 0] \cdot A_{LN})^T \tag{2.20}$$

The relative velocity can be calculated by simply subtracting the two

$$\begin{aligned} \vec{V}_{r_N} &= \vec{v}_N - \vec{v}_{atm} \\ \vec{V}_{r_B} &= A_{BN} \cdot \vec{V}_{r_N} \end{aligned} \tag{2.21}$$

2.3.5 Magnetic field $\vec{B}$

The Earth's magnetic field was simulated accordingly to the World Magnetic Model [5] [9].

Firstly, the magnetic field $\vec{b}_{ER}$ is computed in a reference frame that rotates with the Earth. $\vec{b}_{ER}$ is the negative of the gradient of a scalar potential V, normally modeled as a series expansion of spherical harmonics.

$$V(r,\theta,\phi) = R \sum_{n=1}^{k} \left(\frac{R}{r}\right)^{n+1} \sum_{m=0}^{n} \left[g_n^m \cos(m\phi) + h_n^m \sin(m\phi)\right] P_n^m(\theta) \tag{2.22}$$

where r, θ and ϕ are the spherical coordinates of the position of the spacecraft, and g_n^m and h_n^m are Gaussian coefficients that can be found in the IGRF 2015 [9].

$$\vec{b}_{ER} = -\nabla V = \begin{cases} b_r = -\dfrac{\partial V}{\partial r} \\ b_\theta = \dfrac{-1}{r}\dfrac{\partial V}{\partial \theta} \\ b_\phi = \dfrac{-1}{r\sin\theta}\dfrac{\partial V}{\partial \phi} \end{cases} \tag{2.23}$$

In the lecture notes [5], the following equations are presented to calculate the above derivatives

$$\begin{aligned} b_r &= \sum_{n=1}^{k}\left(\frac{R}{r}\right)^{n+2}(n+1)\sum_{m=0}^{n}\left[g^{n,m}\cos(m\phi)+h^{n,m}\sin(m\phi)\right]P^{n,m}(\theta) \\ b_\theta &= -\sum_{n=1}^{k}\left(\frac{R}{r}\right)^{n+2}\sum_{m=0}^{n}\left[g^{n,m}\cos(m\phi)+h^{n,m}\sin(m\phi)\right]\frac{\partial P^{n,m}}{\partial\theta}(\theta) \\ b_\phi &= \frac{-1}{\sin\theta}\sum_{n=1}^{k}\left(\frac{R}{r}\right)^{n+2}\sum_{m=0}^{n} m\left[-g^{n,m}\sin(m\phi)+h^{n,m}\cos(m\phi)\right]P^{n,m}(\theta) \end{aligned} \tag{2.24}$$

where the unknown terms can be computed as in [5].

To get the magnetic field in the Earth-centered inertial frame, one simply has to do the following calculation

$$\vec{b}_N = \begin{bmatrix} b_1 \\ b_2 \\ b_3 \end{bmatrix} = \begin{cases} b_1 = [b_r\cos(\delta)+b_\theta\sin(\delta)]\cos(\alpha) - b_\phi\sin(\alpha) \\ b_2 = [b_r\cos(\delta)+b_\theta\sin(\delta)]\sin(\alpha) + b_\phi\cos(\alpha) \\ b_3 = b_r\sin(\delta) - b_\theta\cos(\delta) \end{cases} \tag{2.25}$$

where $\delta = \phi/2 - \theta$ is the satellite declination, and $\alpha = \phi + \alpha_G$ with α_G being the Greenwich meridian right ascension.

Since the orbit is geostationary, the spacecraft will always measure the same magnetic field. Therefore, in order for the system to be observable, one more sensor needs to be used. The Earth horizon sensor was used for that reason.

2.3.6 Earth horizon vector $\vec{EH}$

The Earth horizon vector is a unitary vector that points to the Earth. It can be measured onboard of the spacecraft with an Earth horizon sensor.

To obtain the real Earth horizon vector, one simply has to use symmetric of the unitary vector $\vec{r}$ from subsection 2.3.2.

$$\vec{EH} = -\vec{r} \tag{2.26}$$

2.4 Disturbances

The considered disturbances were: gravity gradient, solar radiation pressure, parasitic magnetic torque, and drag.

2.4.1 Gravity gradient

A derivation of the equations is present in the lecture notes [5]. The final equations that were used to model the disturbance torque caused by the gravity gradient were

$$u_{d\ x}^{\mathrm{gg}} = 3n^2(I_z - I_y)c_3c_2 \tag{2.27}$$
$$u_{d\ y}^{\mathrm{gg}} = 3n^2(I_x - I_z)c_1c_3 \tag{2.28}$$
$$u_{d\ z}^{\mathrm{gg}} = 3n^2(I_y - I_x)c_2c_1 \tag{2.29}$$

where n is the orbital angular velocity and c_1, c_2 and c_3 are the direction cosines of the radial direction in the principal axes. Recalling the $\vec{r}$ defined in subsection 2.3.2, then c_i corresponds to its coordinates in the body frame

$$\begin{bmatrix} c_1 & c_2 & c_3 \end{bmatrix}^T = \vec{r}_B \tag{2.30}$$

2.4.2 Solar radiation pressure

The solar radiation pressure is a disturbance torque caused by the incident radiation on the spacecraft. The force in each surface can be calculated as [5]

$$\vec{F}_i^{\mathrm{srp}} = PA\left(\hat{S}\cdot\hat{n}_i\right)\left[(1-\rho_s)\,\hat{S} + \left(2\rho_s\left(\hat{S}\cdot\hat{n}_i\right) + \frac{2}{3}\rho_d\right)\hat{n}_i\right] \tag{2.31}$$

where $\hat{S}$ is the Sun vector and $\hat{n}_i$ is the normal vector of each surface. In the simulation, it was used $\hat{S}$ and $\hat{n}_i$ written in the body reference frame, in order to get the force also written in the body reference frame. Since the spacecraft is cuboid shaped, then the normal vectors are

$$\begin{aligned} \hat{n}_1 &= [1 \quad 0 \quad 0] & \hat{n}_2 &= [0 \quad 1 \quad 0] & \hat{n}_3 &= [0 \quad 0 \quad 1] \\ \hat{n}_4 &= [\text{-}1 \quad 0 \quad 0] & \hat{n}_5 &= [0 \quad \text{-}1 \quad 0] & \hat{n}_6 &= [0 \quad 0 \quad \text{-}1] \end{aligned} \tag{2.32}$$

To obtain the produced torque

$$\vec{u}_d^{\mathrm{srp}} = \begin{cases} \sum_{i=1}^{n} \vec{c}_{p\,i} \times \vec{F}_i^{\mathrm{srp}} & ,\hat{S}_b\cdot\hat{n}_i > 0 \\ 0 & ,\hat{S}_b\cdot\hat{n}_i \leq 0 \end{cases} \tag{2.33}$$

where $\vec{c}_{p\,i}$ is the vector from the spacecraft's center of mass to the surface's geometric center.

Notice how the assumed homogeneous cuboid shaped spacecraft wouldn't suffer any disturbance since the surfaces' geometric centers would be aligned with the center of mass. In order to simulate the solar radiation pressure, the center of mass was assumed to be 1% off-centered in each axis.

2.4.3 Parasitic magnetic torque

The interaction between the Earth's magnetic field and the spacecraft's local magnetic fields, induced by the flow of current, causes a disturbance torque. This parasitic disturbance torque can be modeled by

$$\vec{u}_d^{\mathrm{m}} = \vec{m} \times \vec{b}_B \tag{2.34}$$

where $\vec{m}$ is the residual magnetic induction, due to currents in the satellite, and can be aproximated by (worst case)

$$\vec{m} = [0.1 \quad 0.1 \quad 0.1]^T\ \mathrm{Am}^2 \tag{2.35}$$

2.4.4 Drag

As mentioned above, the atmospheric drag can be neglected for a geostationary orbit. Nonetheless, the computation was implemented in order for the model to be applicable to different orbits.

The force on each spacecraft's surface caused by the atmosphere can be computed by

$$\vec{F}_{i_B}^{\text{drag}} = -\frac{1}{2} C_D \rho \vec{V}_{r_B} \left(\vec{V}_{r_B} \cdot \vec{n}_i \right) A_i \tag{2.36}$$

The disturbance torque is computed in a similar way to the case of solar radiation pressure

$$\vec{u}_d^{\text{drag}} = \begin{cases} \sum_{i=1}^{n} \vec{c}_{p\,i} \times \vec{F}_i^{\text{drag}} & , \vec{V}_{r_B} \cdot \hat{n}_i > 0 \\ 0 & , \vec{V}_{r_B} \cdot \hat{n}_i \leq 0 \end{cases} \tag{2.37}$$

2.5 Sensors

2.5.1 Gyroscope

The gyroscope measures the spacecraft's angular velocities. However, the measurements contain some noise that can be modeled as

$$\begin{aligned} \vec{w}_m &= \vec{w} + \vec{n} + \vec{b} \\ \vec{n} &\sim G(0, \sigma_n) \\ \dot{\vec{b}} &\sim G(0, \sigma_b) \end{aligned} \tag{2.38}$$

where $\vec{\omega}_m$ is the angular velocity measurements and G is white Gaussian noise with zero mean and standard deviation σ_n and σ_b.

The noise n is known as angular random walk (ARW) and is attributed to thermal mechanical noise of the system. The standard deviation can be calculated as

$$\sigma_n = \frac{ARW}{\sqrt{T_s}} = \frac{0.15 \frac{\pi}{180} \frac{1}{\sqrt{3600}}}{\sqrt{\frac{1}{262}}} \simeq 7.0627 \times 10^{-4}\,\text{rad} \tag{2.39}$$

where $T_s = \frac{1}{f_s}$ is the sampling time. Notice how ARW needs to be converted to the correct units.

The noise b is known as rate random walk (RRW) and is attributed to electronic noise (flicker). The standard deviation can be calculated as

$$\sigma_b = \frac{RRW}{\sqrt{T_s}} = \text{bias instability} = 0.3 \frac{\pi}{180} \frac{1}{3600} \simeq 1.4544 \times 10^{-6}\,\text{rad} \tag{2.40}$$

To model the gyroscope's sampling frequency, a block zero-order hold was used.

The measured angular velocities are very noisy and therefore are later filtered. The filtering will be described below.

2.5.2 Magnetometer

The magnetometer was modeled with an accuracy of 5°. To model the error, the following matrix was used

$$A_\varepsilon = \begin{bmatrix} \cos\varepsilon\cos\varepsilon & \cos\varepsilon\sin\varepsilon\sin\varepsilon + \sin\varepsilon\cos\varepsilon & -\cos\varepsilon\sin\varepsilon\cos\varepsilon + \sin\varepsilon\sin\varepsilon \\ -\sin\varepsilon\cos\varepsilon & -\sin\varepsilon\sin\varepsilon\sin\varepsilon + \cos\varepsilon\cos\varepsilon & \sin\varepsilon\sin\varepsilon\cos\varepsilon + \cos\varepsilon\sin\varepsilon \\ \sin\varepsilon & -\cos\varepsilon\sin\varepsilon & \cos\varepsilon\cos\varepsilon \end{bmatrix} \tag{2.41}$$

$$\vec{b}_{m_B} = A_\varepsilon \cdot \vec{b}_B \tag{2.42}$$

where ε is the sensor accuracy and $\vec{b}_B$ is the magnetic field vector in the body reference frame.

2.5.3 Earth horizon sensor

The modeling of the Earth horizon sensor is identical to the magnetometer. A matrix A_ε is used with an accuracy of 6 arcminutes. The measured Earth horizon vector corresponds to

$$\vec{EH}_{m_B} = A_\varepsilon \cdot \vec{EH}_B \tag{2.43}$$

2.5.4 Gyroscope noise filtering

As mentioned and described before, the measurements obtained from the gyroscope are noisy. Nonetheless, a linear observer can be used to filter the noise. For a system of the form

$$\begin{aligned} \dot{\underline{x}} &= f\left(\underline{x}, \underline{u}\right) + \underline{w} \\ \underline{y} &= g\left(\underline{x}\right) + \underline{v} \end{aligned} \tag{2.44}$$

with noises $\underline{w}$ and $\underline{v}$, the liner observer is of the form

$$\dot{\hat{\underline{x}}} = f\left(\hat{\underline{x}}, \hat{\underline{u}}\right) + L\left(\underline{y} - \hat{\underline{y}}\right) \tag{2.45}$$

$$\hat{\underline{y}} = g\left(\hat{\underline{x}}\right) \tag{2.46}$$

Applying the linear observer to the gyroscope, one obtains

$$\dot{\vec{\omega}}_f = J^{-1}\left(J\vec{\omega}_f \times \vec{\omega}_f + \vec{u}_{c_e}\right) + L\left(\vec{\omega}_m - \vec{\omega}_f\right) \tag{2.47}$$

where $\vec{\omega}_f$ is the filtered angular velocity, $\vec{u}_{c_e}$ is the estimated control torque, L is a gain matrix, and $\vec{\omega}_m$ is the measurement from the gyroscope. The gain was chosen to be

$$L = 0.5 \cdot J^{-1} \tag{2.48}$$

where the moment of inertia J was used to tune the response. If the torque was equal in all axes, then the angular velocity would change quicker in the axes with a lower moment of inertia. With the inverse of J, the observer is more sensitive in those axes.

The initial condition used for Eq. 2.47 was

$$\vec{\omega}_{f_0} = \vec{\omega}_m|_{t=0} \tag{2.49}$$

2.5.5 Attitude determination

To obtain the attitude of the spacecraft, a dynamic method for attitude determination is used, more specifically, a nonlinear observer.

Based on the lecture notes [5], the following observer was implemented

$$
\begin{aligned}
\frac{d\hat{q}}{dt} &= \frac{1}{2} \cdot \Omega(\vec{\omega}_f + \vec{\alpha}) \cdot \hat{q} \\
\Omega(\vec{x}) &= \begin{bmatrix} 0 & x_3 & -x_2 & x_1 \\ -x_3 & 0 & x_1 & x_2 \\ x_2 & -x_1 & 0 & x_3 \\ -x_1 & -x_2 & -x_3 & 0 \end{bmatrix} \\
\alpha &= \sum_{i=1}^{n} k_i \left(\vec{a}_{Bi} \times \hat{A} \cdot \vec{a}_{Ni} \right) \\
k_i = 10 \cdot \left[\frac{e_h}{e_m + e_h} \quad , \quad \frac{e_m}{e_m + e_h} \right] \quad a_{Bi} &= \left[\vec{b}_{m_B} \quad , \quad \vec{EH}_{m_B} \right] \qquad a_{Ni} = \left[\vec{b}_N \quad , \quad \vec{EH}_N \right]
\end{aligned}
\tag{2.50}
$$

where $\hat{q}$ is the estimated quaternion, $\hat{A}$ is an estimation of the DCM matrix obtained with $\hat{q}$, and the vector k_i is an array of the normalized inverse of the sensors' accuracy times 10.

The initial estimated quaternion $\hat{q}_0$ was chosen to be a random vector of 4 elements and norm 1. However, for slightly faster results, one could use an estimative obtained by the TRIAD method [5], for example.

As previously implemented, the derivative was normalized in each iteration for better results. The quaternion was also converted to the DCM representation in order to calculate α.

2.6 Controller

2.6.1 De-tumble controller

The implemented control law was

$$
\vec{u}_c = -J\vec{\omega}_f \times \vec{\omega}_f - k_1 \cdot J\vec{\omega}_f \tag{2.51}
$$

This control law grants asymptotic stability when there are no disturbances. Since the disturbances experienced by the spacecraft are very small, this control law does a good job to de-tumble the spacecraft. The initial term is not necessary but helps with the dynamics of the spacecraft.

Having in mind the actuators for this phase of the mission, the gain k_1 was chosen to be

$$
k_1 = 1 \cdot \frac{T_{max}}{\omega_{lb}} \tag{2.52}
$$

where T_{max} is the maximum possible torque produced by the thrusters and ω_{lb} is the angular velocity at which the controller switches to the slew maneuver.

Having the ideal control torque, the controller still has to compute which thrusters to turn on in order to approximate that desired torque. To do so, a projective control was implemented.

Essentially, a table is made with all the 16 possible combinations of the 4 thrusters and their resultant torque. Then, the selected thrusters correspond to the combination that minimizes a defined cost function.

$$
J_n = \|\vec{u}_{ideal} - \vec{u}_n\| \tag{2.53}
$$

where $\vec{u}_{ideal} = \vec{u}_c$ and $\vec{u}_n$ corresponds to each entry of the look-up table.

The controller returns an array with which thrusters to turn on or off.

2.6.2 Slew maneuver and tracking controller

The implemented control law was

$$\begin{aligned}
\vec{u}_c &= -J\vec{\omega}_f \times \vec{\omega}_f - k_{2\omega} J\vec{\omega}_f + k_{2q} J \frac{\partial H}{\partial q_{4e}}(\hat{q}_{4e})\underline{q}_e \\
\underline{q}_e &= \begin{bmatrix} q_{d\,4} & q_{d\,3} & -q_{d\,2} & -q_{d\,1} \\ -q_{d\,3} & q_{d\,4} & q_{d\,1} & -q_{d\,2} \\ q_{d\,2} & -q_{d\,1} & q_{d\,4} & -q_{d\,3} \\ q_{d\,1} & q_{d\,2} & q_{d\,3} & q_{d\,4}]; \end{bmatrix} \cdot \hat{q}
\end{aligned} \tag{2.54}$$

where q_d is the desired quaternion.

Like in the previous controller, it is also asymptotically stable.

In this controller, the implemented H function was

$$H(q_{4e}) = 1 - |q_{4e}| \tag{2.55}$$

$$\frac{\partial H}{\partial q_{4e}}(\hat{q}_{4e}) = -\text{sign}(q_{4e}) \tag{2.56}$$

which doesn't have unwinding problems.

According to the lecture notes [5], to obtain a critically damped response for the given H function, the gains have to relate through

$$\begin{aligned}
J\dot{\vec{\omega}} &= -k_{2\omega} J\vec{\omega} + k_{2q} J \frac{\partial H}{\partial q_{4e}}(q_{4e})\underline{q}_e \\
\Rightarrow \ddot{\theta} + k_{2\omega}\dot{\theta} - \frac{k_{2q}}{2}\frac{\partial H}{\partial q_{4e}}(q_{4e})\theta &= 0 \\
\Rightarrow k_{2\omega}^2 &= 2k_{2q}
\end{aligned} \tag{2.57}$$

In the applied controller, the selected gains were

$$k_{2\omega} = 0.1 \qquad\qquad k_{2q} = \frac{k_{2\omega}^2}{2} = 0.005 \tag{2.58}$$

Having the desired control torque, the controller has to compute how to vary the reaction wheels to produce that torque.

$$\begin{aligned}
\vec{u}_c &= -\vec{\omega} \times A\vec{h}_r - A\dot{\vec{h}}_r \\
\Rightarrow \dot{\vec{h}}_r &= -A^*(\vec{u}_c + \vec{\omega} \times A\vec{h}_r)
\end{aligned} \tag{2.59}$$

where $\vec{h}_r$ is a vector with the reaction wheels angular momenta, A is a matrix which columns are the directions of the wheels' axes of rotation, and A^* is the pseudo-inverse matrix of A (in the case of only 3 RW, it's a simple inverse).

A more detailed explanation of the above equations will be presented at the Actuators section.

2.6.3 Switching controllers

The switching of the controllers is very simple.

The initial selected controller is the de-tumble one. It switches to the slew maneuver and tracking controller when all the angular velocities are less than $\omega_{lb} = 1\,^\circ/\text{s}$

The slew controller switches to the de-tumble controller when any angular velocity is greater than $\omega_{ub} = 10\,^\circ/\text{s}$.

2.7 Actuators

2.7.1 CG thrusters

The torque produced by each thruster is simply

$$\vec{T_i} = \vec{r_i} \times \vec{F_i}$$
$$\vec{u_c} = \begin{cases} \sum_{i=0}^{N} \vec{T_i} & \text{, if thruster } i \text{ is on} \\ 0 & \text{, if thruster } i \text{ is off} \end{cases} \tag{2.60}$$

$\vec{r_i}$ corresponds to the columns of a matrix with the thrusters' positions (with respect to the center of mass) and $\vec{F_i}$ the acting force on the spacecraft.

$$\vec{r_i} = \begin{bmatrix} -d & d & d & -d \\ -d & -d & d & d \\ \frac{c}{2} & \frac{c}{2} & \frac{c}{2} & \frac{c}{2} \end{bmatrix}$$
$$\vec{F_i} = -F_t \begin{bmatrix} -\cos(\alpha) & \cos(\alpha) & \cos(\alpha) & -\cos(\alpha) \\ -\sin(\alpha) & -\sin(\alpha) & \sin(\alpha) & \sin(\alpha) \\ 0 & 0 & 0 & 0 \end{bmatrix}$$

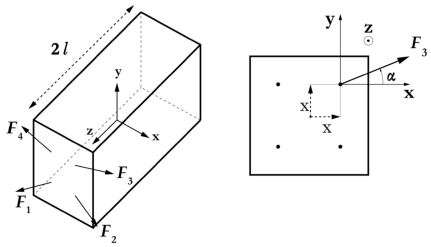

Figure 2.2: Location of the thrusters in the spacecraft [5].

where d is half the distance between two consecutive thrusters and c is the length of the spacecraft along the z-axis. Notice how $\vec{F_i}$ has a negative sign because the forces caused by the thrusters have an opposite direction of the thrusters expel direction (Fig. 2.2).

The result of the above equation corresponds to the selected entry of the thrusters look-up table.

The minimum impulse bit (MIB) of the thrusters was simulated with a block of zero-order hold with sampling time

$$t_s = \frac{\text{MIB}}{F_t} \tag{2.61}$$

2.7.2 Reaction wheels

When a spacecraft has reaction wheels, the total angular momentum is

$$\vec{h} = J\vec{\omega} + A\vec{h_r} \tag{2.62}$$

where the matrix A is a matrix which columns represent the directions of the axes of rotation of the wheels, and h_r is a vector which elements correspond to the angular momentum of each reaction wheel.

Taking the derivative for the particular case of reaction wheels

$$J\dot{\vec{\omega}} + \vec{\omega} \times J\vec{\omega} + A\dot{\vec{h}}_r + \vec{\omega} \times A\vec{h_r} = \vec{T} \tag{2.63}$$

From the above equation, it's clear that the torque applied on the spacecraft by the reaction wheel is

$$\vec{u_c} = -\vec{\omega} \times A\vec{h_r} - A\dot{\vec{h}}_r \tag{2.64}$$

The dynamics of the reaction wheels are described by

$$\vec{T_r} = \dot{\vec{h}}_r = I_r \dot{\vec{\omega}}_r \tag{2.65}$$

where I_r is the moment of inertia of the wheels and $\vec{\omega}_r$ is the angular speed.

Essentially, the controller computes the derivative $\dot{\vec{h}}_r$, the kinematics of the reaction wheels are simulated and then the produced torque on the spacecraft is calculated with Eq. 2.64.

However, the reaction wheels have some physical constraints, which are a maximum angular momentum and a maximum torque. These constraints were modeled with a saturation block applied to $\dot{\vec{h}}_r$ before computing the kinematics of the RW, and another saturation block applied to $\vec{h}_r$ before computing the actual real torque on the spacecraft.

In real scenarios, there's the possibility of the RW getting saturated. When that happens, that RW doesn't deliver torque anymore. To avoid that, the RW must be de-saturated. Essentially, this consists in applying a torque in the wheel proportional to the negative of its angular momentum

$$\vec{T_r} \propto -\vec{h}_r \tag{2.66}$$

However, this will produce a torque in the spacecraft in the opposite direction. Another actuator must be used to counteract that, applying a thrust on the spacecraft equal or proportional to the one applied to the reaction wheel.

$$\vec{T_{sc}} \propto \vec{T_r} \tag{2.67}$$

In the case where those torques aren't equal, then the second actuator needs to run more time in order to de-tumble the spacecraft, due to angular velocities induced by that mismatch.

2.7.3 Estimated control torques

An estimation of the control torques is also computed to later use in the filtering of the gyroscope, which improves its accuracy.

The torque produced by the thrusters is accurately estimated with Eq. 2.60. The torque produced by the reaction wheels is estimated with Eq. 2.64, but with the filtered angular velocity ω_f.

Chapter 3

Results

A simulation was run during 600 s = 10 min and it intended to simulate the de-tumbling, slew maneuver and tracking of the spacecraft. The initial angular velocity was defined as in Eq. 3.1, which corresponds to a vector with norm 30 °/s and direction according to the numerator. The initial attitude quaternion was defined as a random vector of 4 elements and norm 1. The desired attitude quaternion was defined as in Eq. 3.2, which corresponds to having the body axes aligned with the inertial frame axes.

$$\vec{\omega}_0 = \frac{[0.5,\ 1,\ 0.1]^T}{\|[0.5,\ 1,\ 0.1]\|} \cdot 30\,^\circ/\mathrm{s} \qquad (3.1) \qquad\qquad q_d = \begin{bmatrix} 0 & 0 & 0 & 1 \end{bmatrix}^T \qquad (3.2)$$

The simulation took about 20 minutes. The slow computation is due to the zero-order hold blocks which set the maximum step size of the simulation. The maximum step was automatically set to 0.001 s, which corresponds to the sampling time of the zero-order hold block used to model the thrusters' MIB.

Figures 3.1, 3.2, 3.3, 3.4 and 3.5 show some of the most important results.

Conclusions

The de-tumbling took around 250 s and then the slew and tracking controller was activated. The final angular velocities and attitude quaternion were

$$\begin{aligned} \vec{\omega} &= [-3.032,\ -4.508,\ 1.742]^T \times 10^{-4}\,^\circ/\mathrm{s} \\ q &= [-0.0509,\ -0.0039,\ 0.0010,\ 0.9987]^T \Rightarrow \begin{cases} \vec{e} \simeq [-0.0195,\ -0.0765,\ -0.9969] \\ \phi \simeq 5.85\,^\circ \end{cases} \end{aligned} \qquad (3.3)$$

Since the desired quaternion was $q_d = [0,\ 0,\ 0,\ 1]$, then the pointing error simply corresponds to the angle of the quaternion when an axis-angle representation is used, as in Eq. 2.6. Therefore, the accuracy of this ADCS system is, approximately, 5.85 °. This may seem a bit high, but since the sensors used for the attitude determination have an accuracy of 6 arcmin and 5 °, then one could expect such overall accuracy. Some ways to increase the system's accuracy would be to use more accurate sensors or to try other attitude determination algorithms.

Notice how the estimated quaternion is symmetric to the real quaternion, but as mentioned before (Eq. 2.11), they are equivalent.

One important note about the thrusters is that they would take a long time to de-tumble the spacecraft if the angular velocity along the z-axis was large. The reason is that the torque produced by the thrusters along that axis is much smaller. To avoid that problem, another thruster configuration should be adopted.

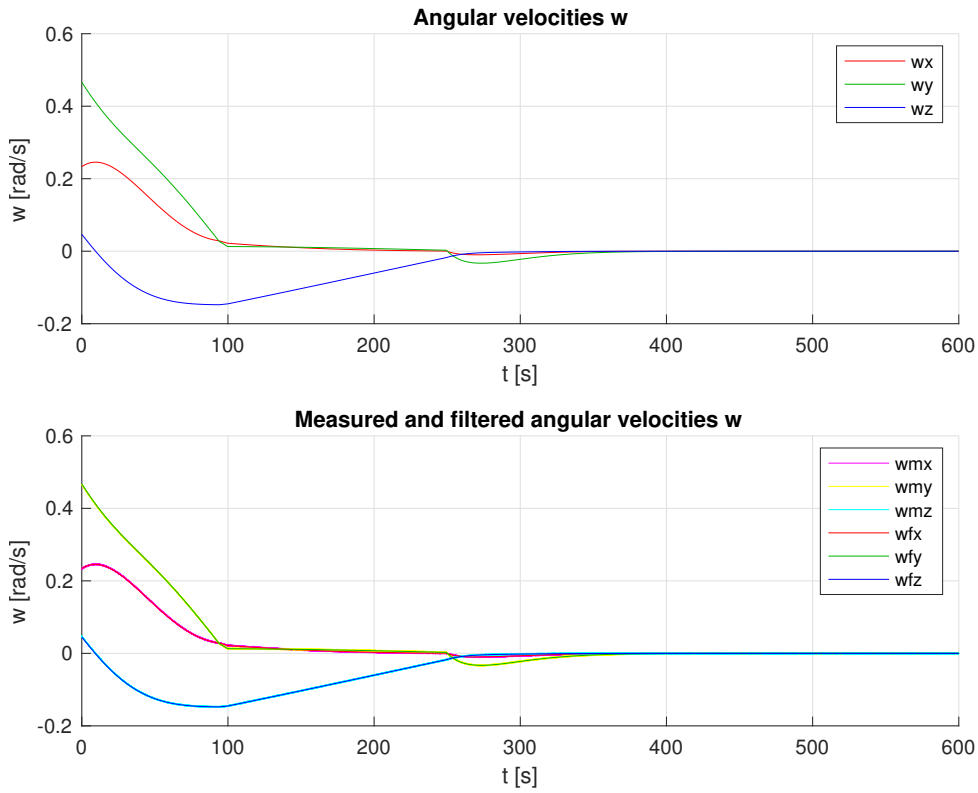

Figure 3.1: Real, measured and filtered angular velocities $\vec{\omega}$.

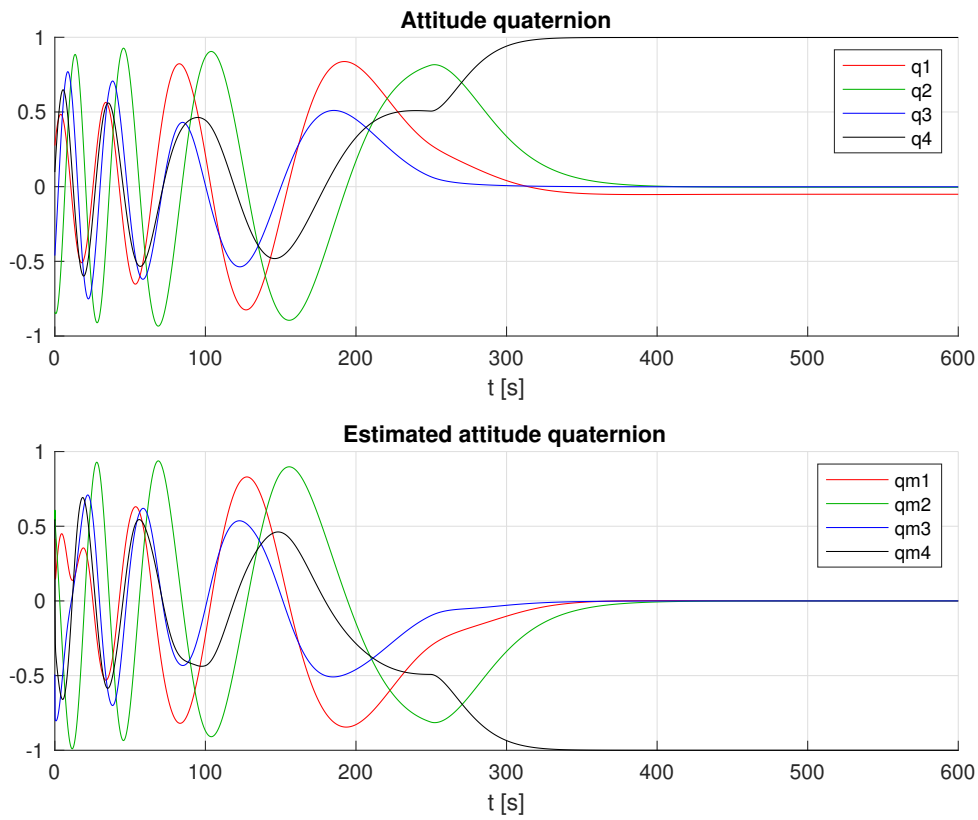

Figure 3.2: Real and estimated attitude quaternions q.

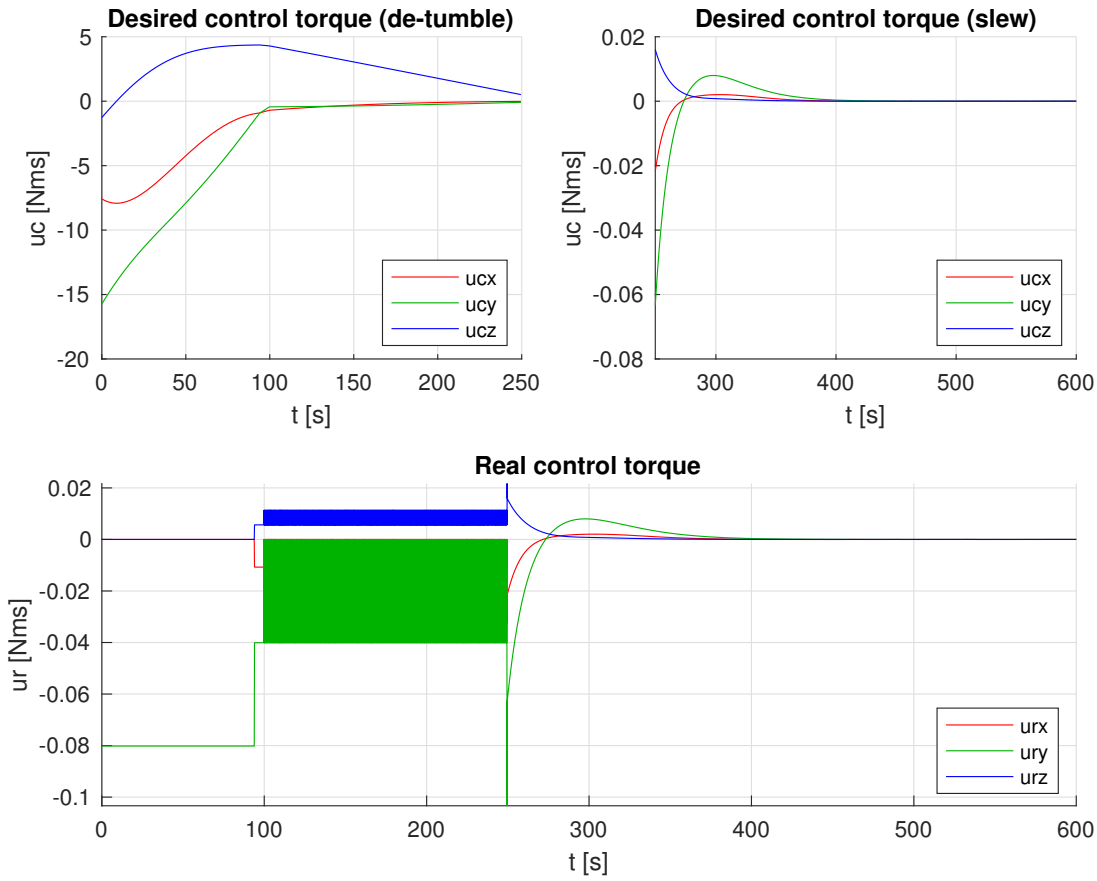

Figure 3.3: Ideal and real control torques.

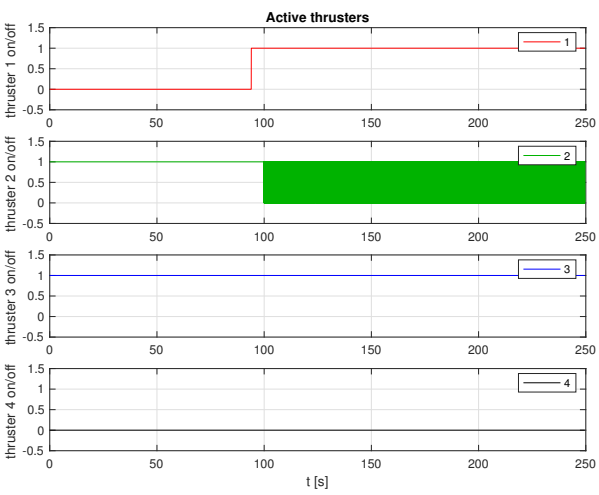

Figure 3.4: Thrusters response.

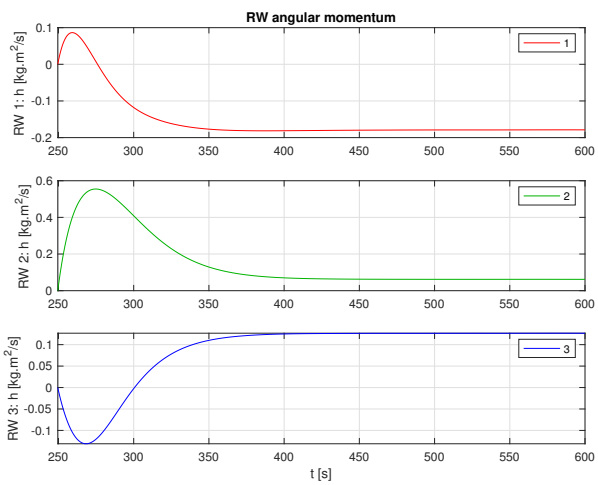

Figure 3.5: Reaction wheels angular momenta.

Bibliography

[1] Defense Industry Daily, "Small is beautiful: Us military explores use of microsatellites." https://www.defenseindustrydaily.com/Small-Is-Beautiful-US-Military-Explores-Use-of-Microsatellites-06720/#definitions, June 2011. Accessed: 5 Jan 2019.

[2] H. J. Kramer, "Proba-v (project for on-board autonomy - vegetation)." https://directory.eoportal.org/web/eoportal/satellite-missions/p/proba-v. Accessed: 12 Dec 2018.

[3] Sensonor, "Sensonor - stim300." https://www.sensonor.com/products/inertial-measurement-units/stim300/. Accessed: 6 Jan 2019.

[4] CubeSatShop, "Nss magnetometer." https://www.cubesatshop.com/product/nss-magnetometer/. Accessed: 10 Jan 2019.

[5] J. D. Biggs, "Lecture notes of spacecraft attitude dynamics and control," 2018.

[6] CubeSatShop, "Mai-ses ir earth sensor." https://www.cubesatshop.com/product/mai-ses-ir-earth-sensor/. Accessed: 10 Jan 2019.

[7] VACCO, "Hybrid adn delta-v / rcs system| vacco industries." https://www.cubesat-propulsion.com/hybrid-adn-delta-v-rcs-system/. Accessed: 6 Jan 2019.

[8] Collins Aerospace, "Rockwell rsi 12 momentum and reaction wheels." https://www.rockwellcollins.com/Products-and-Services/Defense/Platforms/Space/RSI-12-Momentum-and-Reaction-Wheels.aspx. Accessed: 10 Jan 2019.

[9] A. Chulliat, S. Macmillan, P. Alken, C. Beggan, M. Nair, B. Hamilton, A. Woods, V. Ridley, S. Maus, and A. Thomson, "The us/uk world Magnetic Model for 2015-2020: Technical Report," tech. rep., National Geophysical Data Center, NOAA, 2015. doi: 10.7289/V5TB14V7.